

Water soluble quantum dots as hydrophilic carriers and two-photon excited energy donors in photodynamic therapy†

Colin Fowley,^a Nikolitsa Nomikou,^b Anthony P. McHale,^a Paul A. McCarron,^a Bridgeen McCaughan^{*a} and John F. Callan^{*a}

Received 5th January 2012, Accepted 17th February 2012

DOI: 10.1039/c2jm00096b

In search of strategies to develop deeply penetrating agents for use in Photodynamic Therapy (PDT), we have devised a Quantum Dot-Rose Bengal conjugate that is effective at producing singlet oxygen upon two-photon irradiation. The CdSe/ZnS Quantum Dot, with its high two photon absorption cross section, serves as a two-photon absorbing antenna and transfers its excited state energy to the attached photosensitiser which engages with molecular oxygen to produce cytotoxic singlet oxygen. Thus, we were able to excite the photosensitiser indirectly, which has an absorption maximum of 565 nm, with two-photon irradiation at 800 nm. Given the tissue penetration depth of 800 nm light is at least four times greater than 565 nm light, this offers the opportunity to access much deeper-seated tumours than is currently possible with pharmaceutically approved photosensitisers. Furthermore, the attachment of the photosensitiser to the hydrophilic quantum dot improved the aqueous solubility of the photosensitiser by 48 fold, thus overcoming another limitation of currently used photosensitisers, that of poor aqueous solubility.

Introduction

Since the early 1990s, Photodynamic Therapy (PDT) has increasingly been used for the treatment of various cancerous and pre-cancerous conditions.^{1–4} In PDT, a photosensitising (PS) drug, light of suitable wavelength and molecular oxygen combine to produce cytotoxic singlet oxygen. The attraction of PDT as a clinical treatment is due to its minimally invasive nature and the ability to control production of the cytotoxic agent selectively upon irradiation. In effect, the photosensitiser acts as a prodrug and only generates cytotoxic singlet oxygen when activated by light of an appropriate wavelength. In a clinical setting, light can be delivered accurately to the desired area (*i.e.* the tumour) by use of a fiberoptic source thus minimising the collateral damage associated with conventional cancer chemotherapeutic drugs. Although traditionally considered as a treatment for superficial skin cancers, PDT is now emerging as an option in the treatment of other cancers such as head and neck, lung, oesophageal, prostate and bladder.⁵ However, two main factors that still prevent current PDT agents enjoying widespread clinical use are: (1) currently approved PS drugs typically absorb in the visible region (below 700 nm) limiting light penetration to only a few

mm. This is appropriate for the treatment of superficial tumours, but unsuitable for deeper seated tumours;⁶ (2) PS molecules are hydrophobic and tend to aggregate in aqueous solution, leading to a reduction in singlet oxygen production.⁷

To address the problem of poor light penetration in PDT, Anti-Stokes emitting nanoparticles offer great potential.^{8,9} These nanoparticles absorb light of a long wavelength and emit their excited state energy at a shorter wavelength. If a PS molecule is in close proximity to the excited nanoparticle, and has an absorption spectrum that overlaps with the nanoparticle emission spectrum, a Förster Resonance Energy Transfer (FRET) channel to the PS is opened up.⁹ The end result of such an energy transfer is excitation of the PS and Reactive Oxygen Species (ROS) production.¹⁰ Semiconductor Quantum Dots (QDs) are one class of nanoparticles that exhibit strong Anti-Stokes emission (in addition to normal Stokes type emission) due to their high two-photon absorption capability.¹¹ Indeed, the two-photon cross section of CdSe/ZnS QDs is in the region of 50,000 Göpert-Mayer (GM) units which is up to three orders of magnitude greater than conventional dye-based PS molecules.¹¹ As a result, dye-based photosensitisers require very high excitation powers, close to the threshold of tissue damage, that limits their use in two-photon excitation PDT.¹² Therefore, using QDs as a two-photon absorbing antenna enables the indirect excitation of the PS with long wavelength light at acceptable excitation powers (Fig. 1).

In addition to their Anti-Stokes emission, QDs have other impressive properties that make them appealing for use as energy

^aDepartment of Pharmacy and Pharmaceutical Sciences, School of Biomedical Sciences, The University of Ulster, Northern Ireland BT52 1SA. E-mail: j.callan@ulster.ac.uk; b.callan@ulster.ac.uk

^bSonidel Ltd., Dublin 5, Republic of Ireland

† Electronic supplementary information (ESI) available. See DOI: 10.1039/c2jm00096b

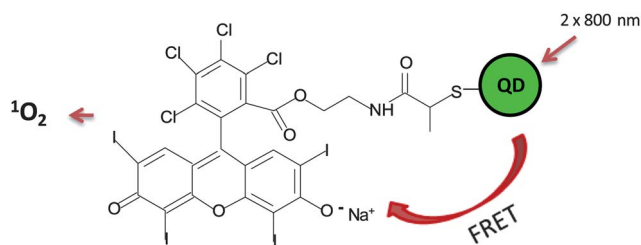


Fig. 1 Schematic representation of how two-photon irradiation at 800 nm leads to singlet oxygen production for **QD-1**.

donors in PDT. For instance, their emission wavelength can be tailored by controlling their size and composition meaning the spectral overlap with PS drugs can be maximised.^{13,14} In addition, their broad absorption spectra offer greater flexibility in the choice of excitation wavelength.^{13,14} Furthermore, their surface can be coated with biocompatible ligands that infer water solubility and permit attachment of small molecules/biomolecules through a range of different chemistries.¹⁵ This feature also offers the opportunity to increase the water solubility of poorly soluble PS drugs through attachment to a hydrophilic QD.

In this manuscript we attach the well known PS drug Rose Bengal to mercaptopropionic acid (MPA) coated CdSe/ZnS QDs. We evaluate the singlet oxygen generating potential of the QD-PS conjugate when irradiated with single and two-photon irradiation, and determine the cytotoxicity of this conjugate using a human tumour cell line. Although several other groups have demonstrated that FRET is possible between QDs and nearby PS drugs,^{7,10,16,17} to the best of our knowledge, no other group has demonstrated the effectiveness of QD-PS conjugates in tumour cell lines or demonstrated the singlet oxygen-generating potential of these conjugates upon two-photon irradiation.

Results and discussion

Synthesis and spectroscopy of the water soluble quantum Dot-Rose Bengal conjugates

CdSe core QDs were prepared according to a procedure developed by Nguyen *et al.*¹⁸ and subsequently coated with a ZnS shell following the procedure developed by Zhu *et al.*¹⁹ The resulting CdSe/ZnS QD were soluble in organic solvents due to their hydrophobic surface ligands and had a quantum yield (ϕ_f) of 36% in chloroform. The hydrophobic ligands were replaced with hydrophilic MPA ligands following a ligand exchange procedure.²⁰ The resulting QD-MPA conjugate was soluble in aqueous PBS buffer (pH = 7.4 ± 0.1) with a ϕ_f of 10%. The UV-Vis spectrum and fluorescence spectrum of QD-MPA were recorded in aqueous solution and show a first exciton peak at 515 nm and an emission λ_{\max} of 535 nm (see supporting information). To enable the conjugation of Rose Bengal to the surface of the QD *via* amide bond formation it was first necessary to functionalise Rose Bengal with an amine group (Scheme 1). This was achieved by the nucleophilic substitution reaction between Rose Bengal sodium salt (RB) and bromoethylamine to form **1** (Scheme 1). The conjugation of **1** to the MPA coated QDs was performed under the assistance of EDC and NHS in a PBS/DMSO solvent (Scheme 1).¹⁵ The resulting conjugate was exhaustively dialysed to purify the **QD-1** conjugates from any unreacted low molecular

weight components. The emission spectrum of the **QD-1** conjugate when excited at 400 nm (a wavelength where the absorption of **1** is negligible but the absorption of the QD is high) is shown in Fig. 2 and reveals only emission from the PS component. The lack of any QD emission at 535 nm in the spectrum of **QD-1** can be attributed to energy transfer from the QD to **1**. For efficient FRET to occur there must be a good overlap between the donor emission spectrum and the acceptor absorbance spectrum. Fig. 3 shows the normalised absorbance spectrum of **1** and the normalised emission spectrum of the MPA coated QDs and reveals a good spectral overlap between the energy donor and acceptor. The efficiency of the FRET process is also known to be distance dependent being proportional to the sixth power of the donor–acceptor distance.^{21,22} Consequently, it is important the QD-PS separation distance is kept to a minimum as QDs are relatively bulky energy donors when compared to their organic counterparts.²² The short spacer used to attach the QD to **1**, limits the donor–acceptor distance in **QD-1** to ~37 Å, based on an average QD diameter of 5.4 nm by TEM (Figure S8), thus helping to improve the FRET efficiency further. The FRET efficiency, E , was calculated using eqn (1)²¹ and was found to be 73% based on an R_0 value of 43.9 Å (R_0 being the donor–acceptor distance at which FRET efficiency is 50% and r the measured donor acceptor distance).

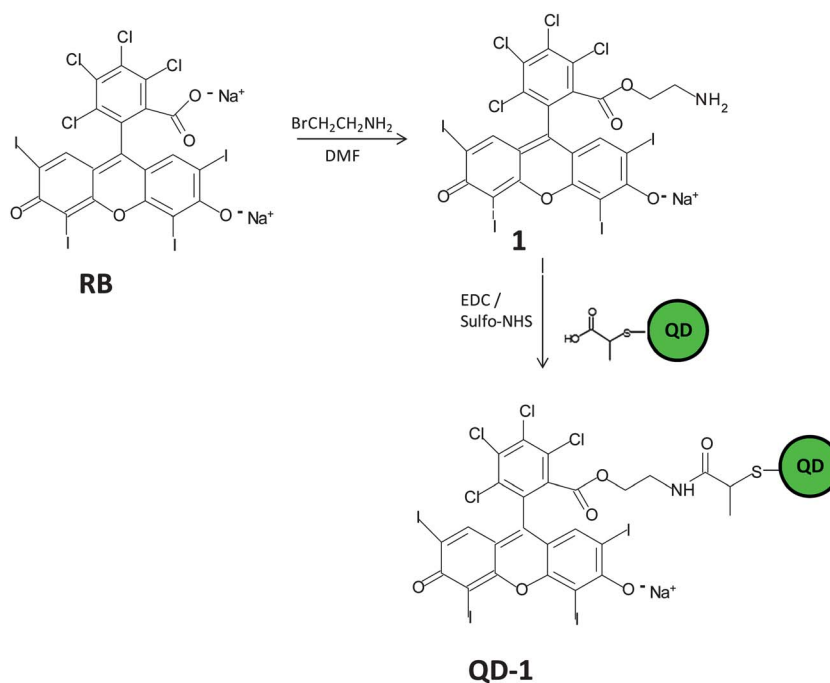
$$E = R_0^6 / R_0^6 + r^6 \quad (1)$$

However, the high loading of **1** on the surface of each QD, calculated as 64 molecules of **1** per QD using UV-Vis spectroscopy, increases the effective acceptor extinction coefficient further, which in turn proportionally improves the effective overlap integral.²¹ Therefore, for FRET systems with more than one acceptor eqn (1)²¹ becomes:

$$E = nR_0^6 / nR_0^6 + r^6 \quad (2)$$

where n is the number of acceptor molecules. Based on 64 PS acceptor molecules being present on the surface of each QD the FRET efficiency (E) now becomes 99.5% illustrating a highly efficient energy transfer process (see ESI† for a detailed calculation of E).

Normally, the conversion of an ionisable primary amine group (such as that present in **1**) to an amide would be accompanied by a drop in aqueous solubility. However, even with a relatively high loading of **1** on the surface of **QD-1**, sufficient MPA groups remained un-reacted to permit aqueous solubility. This dramatic increase in the water solubility before and after conjugation of **1** to the QD surface is illustrated in Fig. 4 where a photograph of **1** and **QD-1** were taken at the same concentration (0.187 mM) in PBS buffer. These photographs reveal **QD-1** as transparent colloidal suspension while the majority of **1** remained un-dissolved. Using a standard calibration curve (UV-Vis) we calculated the increase in the aqueous solubility of **1** to be 48 times greater after incorporation onto the QD surface. In addition, the **QD-1** conjugate displayed excellent long-term stability in aqueous buffer with no evidence of aggregation observed over a 2 month period (see ESI). Good colloidal stability of **QD-1** was supported by a zeta potential measurement of −47.1 mV with the hydrodynamic diameter determined as 9.85 nm (see Figure S8).



Scheme 1 Synthesis of ligand **1** and its incorporation onto MPA coated QDs to form conjugate **QD-1**.

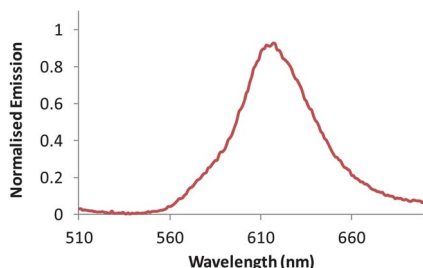


Fig. 2 Normalised emission spectrum of **QD-1** recorded in a PBS solution excited at 400 nm.

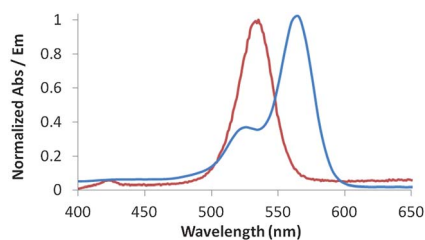


Fig. 3 Normalised absorbance spectrum of **1** (blue line) and emission spectrum of MPA coated QDs (red line).

In vitro singlet oxygen production of **QD-1**

To determine the potential of the **QD-1** conjugate to produce singlet oxygen we utilized the photo-oxidation of 1,3-diphenylisobenzofuran (DPBF) as a quantitative method.²³ In this absorption spectrophotometric assay, DPBF is oxidised to its corresponding diketone upon interaction with singlet oxygen in stoichiometric equivalents. The resulting loss in the DPBF absorbance at 410 nm provides a measure of singlet oxygen production. We irradiated an EtOH:H₂O (50 : 50) solution



Fig. 4 Photograph of **1** (left vial) and **QD-1** (right vial) in PBS buffer at pH 7.4. [**1**] = [**2**] = 0.187 mM.

containing **QD-1** (5 μ M) and DPBF (10 μ M) with 400 nm light delivered from a fibre optic probe (20 J cm⁻²) for 60 min with samples removed and measured every 5 min. Fig. 5 shows a plot of DPBF absorbance at 410 nm against time for **QD-1** and **1** (which was recorded under identical conditions as **QD-1**) and shows a significant reduction in DPBF absorbance for **QD-1** (23%) with only a minor reduction for **1**. Controls for **1** and **QD-1** in the absence of light (Fig. 5) and DPBF with light alone *i.e.* no

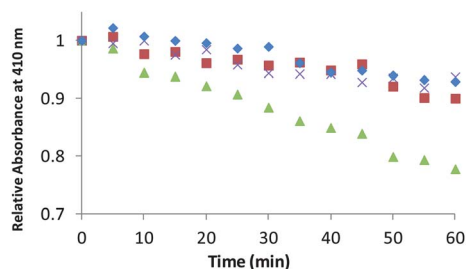


Fig. 5 (a) Plot of relative absorbance of DPBF at 410 nm against time for **1** without irradiation at 400 nm (blue diamonds), **1** with irradiation at 400 nm (red squares), **QD-1** without irradiation at 400 nm (purple crosses) and **QD-1** with irradiation at 400 nm (green triangles). [1] = [QD-1] = 10 μM, DPBF = 10 μM.

1 or **QD-1** (data not shown) produced no significant decrease in the absorbance of DPBF. QDs by themselves have also been proven to generate singlet oxygen in organic solvents albeit with a very low quantum yield.¹⁷ Therefore, to prove that the significant reduction in the absorbance of DPBF for **QD-1** was indeed due to the sensitised excitation of the PS and not due to the direct excitation of the QD, we performed the experiment under identical conditions using MPA coated QDs instead of **QD-1** (see supporting information). We found no evidence of singlet oxygen production for the QDs alone confirming the requirement of an attached PS to enable singlet oxygen generation through a FRET mechanism. In addition, as cancerous tissue vasculature has been shown to be slightly more acidic than normal tissue, with extracellular pH values of approximately 6.8 and 7.4 respectively,²⁴ we incubated the **QD-1** conjugate in PBS buffer at pH 6.8 and observed no evidence of aggregation or precipitation. Furthermore, its ability to produce singlet oxygen was unaffected at this lower pH with the % reduction in DPBF absorbance being identical (23%) after 60 min compared to pH 7.4 (see Figure S9). Therefore, **QD-1** is both stable and effective at producing singlet oxygen at pH 6.8 and pH 7.4.

Cytotoxicity of QD-1 against a human tumour cell line

To determine if the singlet oxygen generated would have the desired cytotoxic effect in tumour cells, we carried out a similar experiment using HeLa cells as a target in a tissue culture-based bioassay. HeLa cells were cultured in 96-well plates and **QD-1**

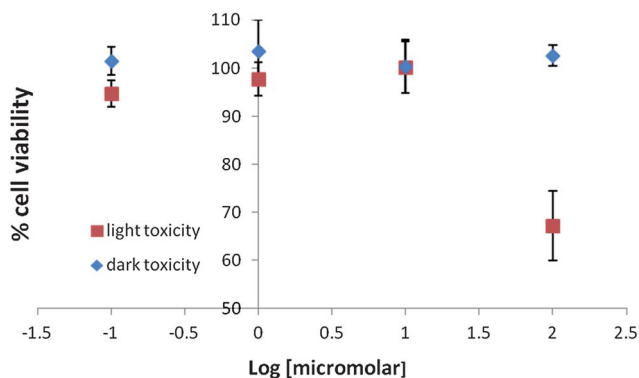


Fig. 6 Plot of cell viability (HeLa cells) against **QD-1** concentration before (blue diamonds) and after (red squares) irradiation at 365 nm.

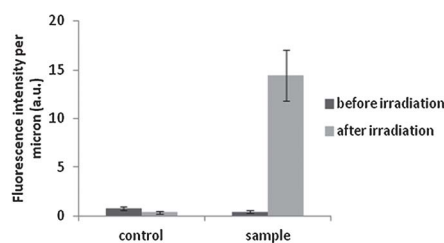
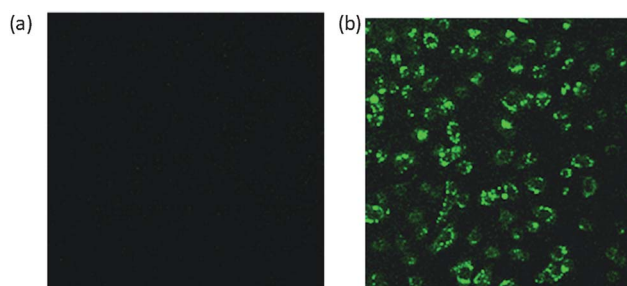


Fig. 7 Confocal fluorescence images of HeLa cells incubated with DHFA and **QD-1** (a) before two-photon irradiation at 800 nm and (b) after two-photon irradiation at 800 nm. (c) Plot of fluorescence intensity per micron of HeLa cell for control cells (incubated with DHFA and exposed to two-photon irradiation) and sample cells (incubated with DHFA + **QD-1** and exposed to two-photon irradiation) before and after irradiation.

was added to selected wells at concentrations of 0, 1, 10 and 100 μM in PBS buffer and incubated for 6 h. at 37 °C. Wells were washed to remove any excess **QD-1**, fresh medium was added to each well and these were then irradiated for 20 min using 365 nm light. In this study, 365 nm irradiation was used instead of 400 nm irradiation, as the 365 nm light source enabled the simultaneous irradiation of all wells in the 96 well plate, and also guaranteed an equal irradiation dose to each well. As before, the QD absorbs strongly at 365 nm while **1** has negligible absorbance. Control cells containing **QD-1** but not subjected to irradiation were also used for comparative purposes and to allow for the determination of any inherent ‘dark’ toxicity due to **QD-1** alone. Following irradiation the cells were incubated for 24 h before the viability was determined using an MTT assay.²⁵ No noticeable dark toxicity was observed for **QD-1** up to a concentration of 100 μM, while a 33% reduction in cell viability was observed at the same concentration upon light irradiation (Fig. 6). Therefore, these results indicate that **QD-1** is cytotoxic toward HeLa cells when irradiated at a wavelength where **1** does not absorb indicating the FRET mechanism is operating effectively in a cellular environment and the generation of singlet oxygen from the indirectly excited PS is causing the desired toxic effect.

Two-photon induced singlet oxygen production of QD-1

To demonstrate the ability of the **QD-1** conjugate to produce singlet oxygen upon two-photon irradiation, we incubated HeLa cells with **QD-1** (100 μM) and the fluorescent singlet oxygen probe 2',7'-dichlorodihydrofluorescein diacetate (DHFA) (8.3 μM). When taken up by HeLa cells, the acetate groups present on DHFA are cleaved by esterase enzymes leaving it

susceptible to oxidation by singlet oxygen, the reduced form of hydrolysed DHLA being non-fluorescent and the oxidised form fluorescent.^{5,26–28} We recorded the confocal fluorescence images of the cells before and after two-photon irradiation at 800 nm for 5 min (Fig. 7a + b). No evidence of any fluorescence was observed for cells treated with DHFA alone, before, or after irradiation (see supporting information). However, for cells treated with both **QD-1** and DHFA there was a significant increase in intensity of fluorescence after two photon irradiation. Indeed, by determining the average intensity of fluorescence per micron across the HeLa cell we were able to quantify the increase in fluorescence to be over 14 times greater for those cells treated with two photon irradiation (Fig. 7c). These results dramatically demonstrate that **QD-1** is effective at producing singlet oxygen upon two photon irradiation in living human tumour cells.

Conclusions

We have conjugated a conventional photosensitising drug, Rose Bengal, with CdSe/ZnS QDs and showed the resulting conjugate can produce significant quantities of singlet oxygen upon both single and two-photon irradiation *via* a FRET mechanism. This offers the opportunity to exploit the excellent penetration depth associated with two photon excitation schemes in biological samples and target deeper seated tumours using PDT. An added benefit of using nanoparticle based photosensitisers in PDT is the Enhanced Permeation and Retention (EPR) effect, whereby nanoparticles tend to accumulate in extra-vascular tumour tissue much more readily than in healthy tissue, thus enhancing tumour targeting.^{26–28} In addition, the potential for improving the aqueous solubility of poorly soluble PS drugs is another significant benefit of utilising QDs as drug carriers. Furthermore, the broad absorption spectra and tuneable emission spectra of QDs, allows them to be used as energy donors with a range of different photosensitisers, potentially improving the efficacy of these compounds. Although there is some concern over the long-term toxicity of cadmium containing QDs *in vivo*, each potential application involving these nanoparticles should be considered on its own merit. For instance, the issue of potential QD toxicity in therapeutic applications such as PDT for the treatment of cancer, must be balanced against the extreme side effects and potential long-term health effects of conventional cancer chemotherapeutic drugs which include nervous system disorders, kidney and liver dysfunction, cardiotoxicity and loss of fertility. Furthermore, as PDT is usually given as a one off treatment, repeated exposure is not an issue. In any case, non-invasive therapies such as PDT are extremely attractive in palliative situations, where extended survival and quality of life must be considered together. We believe QDs have a future in two-photon excited PDT and that their potential toxicity can be limited by controlling factors such as nanoparticle composition, hydrodynamic diameter, the use of biocompatible coatings and control of the surface charge.²⁹

Experimental

Materials and methods

Chemicals were purchased from commercial sources at the highest possible purity and used as received. NMR spectra were

recorded on a Varian 500 MHz NMR spectrometer. Mass spectra were recorded on a LCQTM quadrupole ion-trap mass spectrometer (Finnigan MAT, San Jose, California, USA) utilising electrospray ionisation (ESI). TEM images were recorded with an FEI Tecnai 12 microscope on copper grids (200 mesh) using a uranyl acetate stain. UV-Vis spectra were recorded with a Varian Cary spectrometer, using quartz cells with a path a length of 1 cm. Emission spectra were recorded with a Varian Cary Eclipse spectrometer in aerated solutions, slits = 5 nm.

Synthesis of 1

To a solution of Rose Bengal sodium salt (1.0 g, 1.0 mmol) in anhydrous DMF (10 mL) was added 2-bromoethylamine (0.32 g, 1.5 mmol) and the mixture was stirred at 80 °C for 7 h. The DMF was then removed under reduced pressure and the residue stirred for 18 h in diethyl ether (200 mL). The solution was filtered and the resulting solid stirred in water (200 mL) for 18 h. The solution was filtered and the solid crystallised from MeOH to yield the product as a dark red solid. ¹H NMR (500 MHz, DMSO-d₆): 2.42 (t, CH₂, 2H), 3.80 (t, OCH₂, 2H), 7.26 (s, ArH, 2H), 7.60 (s, NH₂, 2H). ¹³C NMR (500 MHz, DMSO-d₆): 19.0, 37.5, 49.3, 56.5, 62.7, 76.6, 97.9, 129.6, 130.6, 132.4, 133.4, 10.6, 110.9, 134.7, 135.7, 136.4, 137.0, 139.6, 157.5, 163.2, 172.3. HRMS: calculated for C₂₂H₉Cl₄I₄NO₂ = 1016.5384, found 1016.1376. I.R. ν_{max} (cm⁻¹) 3430, 2925, 2366, 1615, 1546, 1450, 1337.

Synthesis of CdSe/ZnS QDs

Cadmium oxide (6.4 mg, 5 mmol), stearic acid (71.0 mg, 25.0 mmol) and octadecane (5.0 mL) were charged to a three necked flask and placed under vacuum for 30 min. The resulting mixture was then heated to 230 °C under argon until the solution became clear. The solution was cooled to 25 °C and hexadecylamine (3.0 g, 12 mmol) added. The flask was placed under vacuum again for 5 min and the contents then heated to 180 °C under argon when the solution turned clear. In a separate flask, a solution of selenium powder (79.0 mg, 0.10 mmol) in trioctylphosphine (TOP) (5 mL) was sonicated until it became clear. The contents of this flask were then injected into the cadmium solution at 180 °C as quickly as possible. The reaction was quenched after 4 min by the addition of cold toluene (40.0 mL). The CdSe core QDs were purified by the addition of MeOH (20 equivalents) and centrifuged at 5000 rpm for 10 min. The MeOH was decanted off and the CdSe QDs re-dispersed in CHCl₃.

The core CdSe QDs were then coated by a ZnS shell following the procedure adopted by Zhu *et al.*¹⁹ Briefly, CdSe QDs (0.15 μmol) in chloroform were placed in a two neck flask and the solvent was removed under vacuum. Octadecylamine (1.50 g, 5.56 mmol) and 1-octadecene (5.0 mL, 15.58 mmol) were added to the flask and the solution heated to 80 °C under reflux. The zinc and sulphur precursors were prepared in separate flasks. The zinc precursor was prepared by heating a mixture of anhydrous zinc acetate (74.0 mg, 0.40 mmol), trioctylphosphine oxide (0.50 g, 1.29 mmol), trioctylphosphine (2.0 mL, 4.48 mmol) and 1-octadecene (5.0 mL) at 200 °C until the solution became clear and then cooled to 25 °C. The sulphur precursor was prepared by dissolving thiourea (60.0 mg, 0.78 mmol) in EtOH (4.0 mL). The zinc precursor (0.75 mL) was then injected into the stirring QD

solution at 80 °C and stirred for 15 min. The sulphur precursor (0.20 mL) was then added and the solution stirred for 10 min. The solution was then cooled to 25 °C and acetone (10 volume equivalents) added. The resulting turbid solution was centrifuged at 5000 rpm for 5 min, the acetone removed and the CdSe/ZnS QDs isolated as yellow/orange solid and re-dispersed in CHCl₃. The CdSe/ZnS QDs were further purified by repeated dissolution in CHCl₃ and precipitation with MeOH.

Synthesis of hydrophilic MPA coated CdSe/ZnS QDs

Following a procedure developed by Pong *et al.*,²⁰ tetramethylammonium hydroxide pentahydrate TMAH (100.0 mg, 0.55 mmol) was mixed with 3-mercaptopropionic acid (MPA) (22.5 µL, 0.28 mmol) in CHCl₃ (1.0 mL). After 1 h, the bottom layer was removed and added to a poly(propylene) tube and CdSe/ZnS QDs (0.10 µM) in a minimum amount of CHCl₃ added. The solution was mixed and allowed to stand at room temperature for 40 h. The MPA coated QDs were isolated as an intensely fluorescent droplet on top of the CHCl₃ and re-dispersed in PBS buffer. The water soluble QDs were used directly in the next step.

Synthesis of QD-1 conjugates

Following a procedure developed by Yildiz *et al.*,¹⁵ MPA coated CdSe/ZnS QDs (0.10 µM) in PBS (3.0 mL) was added to EDC (5.7 mg, 30 µM) and sulfo-NHS (2.0 mg, 10 µM) added. The solution was stirred at 25 °C for 20 min. Amine Rose Bengal (10.0 mg, 10.0 µM) dissolved in DMSO (2.0 mL) was added and the solution stirred for 4 h. The contents were repeatedly dialysed against ACN/water (50 : 50) using a 12,000 MW cut off dialysis tubing. The contents of the dialysis tubing were placed in a beaker and diluted with PBS buffer (pH 7.4 ± 0.1) to acquire a (50 : 50 v/v) H₂O/PBS solution.

In vitro singlet oxygen determination

A solution was prepared containing QD-1 (5 µM) and DPBF (10 µM) in EtOH:H₂O (50 : 50 v/v). The solution was aerated for 10 min before being irradiated for 60 min with light of 400 nm delivered from a fibre optic probe (20 J cm⁻²). Aliquots were removed and their absorbance recorded every 5 min at 410 nm using a Carey Absorbance spectrometer.

Cell viability studies

HeLa cells were cultured in DMEM, supplemented with foetal bovine serum (10% v/v) penicillin (200 U mL⁻¹), streptomycin (200 µg mL⁻¹) and non-essential amino acids (0.1 mM). The cells were seeded in 96 well plates at a density of 5 × 10⁴ cells mL⁻¹, incubated overnight at 37 °C in O₂/CO₂/air (20 : 5 : 75, v/v/v) and spiked with amounts of QD-1 prepared in a PBS:H₂O (50 : 50 v/v) solution to allow for final concentrations of 0.1, 1.0, 10.0 and 100 µM. The cells were incubated in the dark for a further 6 h, after which all cell medium was removed and each well washed twice with 200 µL PBS. A 100 µL volume of fresh PBS was added to each well and the plate subjected to 20 min irradiation at 365 nm using an UVP UVGL-58 lamp (0.4 mW cm⁻²). After irradiation the PBS was removed and replaced with

100 µL media solution. The cells were allowed to incubate in the dark for a further 24 h at 37 °C in O₂/CO₂/air (20 : 5 : 75, v/v/v). After this time 10 µL (3-(4,5-dimethylthiazol-2-yl)-2,5-diphenyltetrazolium bromide (MTT) solution (5 mg mL⁻¹ PBS) was added to each well. The plates were stored as previously described for 4 h before 85 µL of medium was removed from each well and replaced with 75 µL DMSO. The absorbance of each well was recorded on a Flex Station plate reader at 540 nm.

Intracellular singlet oxygen generation upon two photon excitation of QD-1

HeLa cells were cultured in DMEM, supplemented with foetal bovine serum (10%, v/v), penicillin (200 U mL⁻¹), streptomycin (200 µg mL⁻¹), non essential amino acids (0.1 mM) and incubated overnight at 37 °C in O₂/CO₂/air (20 : 5 : 75, v/v/v). The cells were seeded at a density of 5 × 10⁴ cells mL⁻¹ onto sterile 22 × 22 mm glass cover slips contained in each well of a 6 well plate and incubated overnight. 100 µM QD-1 was added to the coverslips with a control containing no QD-1. The cells were incubated under identical conditions for a further 24 h after which time the QD-1 containing medium was removed and the cells washed three times with PBS (1.0 mL). PBS (2.0 mL) containing 2,7-dichlorodihydrofluorescein diacetate (DHFA) (8.2 µM) was added to each well and the cells incubated for a further 15 min. The DHFA containing PBS was removed from each well and replaced with 2.0 mL fresh medium solution. After incubating for 30 min at 37 °C the cover slips were removed from the well plates, washed twice with PBS (1.0 mL) and imaged with an inverted Leica SP5 confocal/multiphoton microscope. Images were captured using an excitation wavelength at 488 nm with emission recorded between 510 to 550 nm. The coverslips were subjected to 5 min two-photon irradiation at 800 nm using a Leica confocal microscope equipped with a mode locked Ti:sapphire laser generating 100 fs wide pulses at a rate of 80 MHz and images collected again using the same settings as above.

Acknowledgements

CF thanks the University of Ulster for a VCRS studentship.

References

- 1 P. Colin, J. Estevez, N. Betrouni, A. Ouzzane, P. Puech, X. Leroy, J. Biserte, A. Villers and S. Mordon, *Progrès en Urologie*, 2011, **21**, 85–92.
- 2 L. M. Davids and B. Kleemann, *Cancer Treat. Rev.*, 2011, **37**, 465–475.
- 3 M. Ethirajan, Y. Chen, P. Joshi and R. K. Pandey, *Chem. Soc. Rev.*, 2011, **40**, 340–362.
- 4 M. Firczuk, M. Winiarska, A. Szokalska, M. Jodlowska, M. Swiech, K. Bojarczuk, P. Salwa and D. Nowis, *Front. Biosci.*, 2011, **16**, 208–224.
- 5 Cancer Research UK website: <http://search.cancerresearchuk.org/search/results.jsp?siteid=0&query=photodynamic+therapy>.
- 6 M. Wainwright, *Color. Technol.*, 2010, **126**, 115–126.
- 7 A. C. S. Samia, S. Dayal and C. Burda, *Photochem. Photobiol.*, 2006, **82**, 617–625.
- 8 L. Y. Ang, M. E. Lim, L. C. Ong and Y. Zhang, *Nanomedicine*, 2011, **6**, 1273–1288.
- 9 D. K. Chatterjee, L. S. Fong and Y. Zhang, *Adv. Drug Delivery Rev.*, 2008, **60**, 1627–1637.

-
- 10 J. M. Tsay, M. Trzoss, L. Shi, X. Kong, M. Selke, M. E. Jung and S. Weiss, *J. Am. Chem. Soc.*, 2007, **129**, 6865–6871.
 - 11 W. Zipfel, R. Williams and W. Webb, *Nat. Biotechnol.*, 2003, **21**, 1368–1376.
 - 12 K. S. Samkoe, A. A. Clancy, A. Karotki, B. C. Wilson and D. T. Cramb, *J. Biomed. Opt.*, 2007, **12**, 034025.
 - 13 J. F. Callan, A. P. De Silva, R. C. Mulrooney and B. McCaughan, *J. Inclusion Phenom. Macrocyclic Chem.*, 2007, **58**, 257–262.
 - 14 J. F. Callan, R. C. Mulrooney, S. Kamila and B. McCaughan, *J. Fluoresc.*, 2008, **18**, 527–532.
 - 15 I. Yildiz, E. Deniz, B. McCaughan, S. F. Cruickshank, J. F. Callan and F. M. Raymo, *Langmuir*, 2010, **26**, 11503–11511.
 - 16 H. D. Duong and J. I. Rhee, *Chem. Phys. Lett.*, 2011, **501**, 496–501.
 - 17 A. Samia, X. Chen and C. Burda, *J. Am. Chem. Soc.*, 2003, **125**, 15736–15737.
 - 18 H. Q. Nguyen, *Adv. Nat. Sci.: Nanosci. Nanotechnol.*, 2010, **1**, 025004.
 - 19 H. Zhu, A. Prakash, D. N. Benoit, C. J. Jones and V. L. Colvin, *Nanotechnology*, 2010, **21**, 255604.
 - 20 B. Pong, B. L. Trout and J. Lee, *Langmuir*, 2008, **24**, 5270–5276.
 - 21 Lakowicz, J. R., Ed.; In *Principles of Fluorescence Spectroscopy*; Plenum Press: New York, 1999;.
 - 22 I. L. Medintz, A. R. Clapp, H. Mattoussi, E. R. Goldman, B. Fisher and J. M. Mauro, *Nat. Mater.*, 2003, **2**, 630–638.
 - 23 S. O. McDonnell, M. J. Hall, L. T. Allen, A. Byrne, W. M. Gallagher and D. F. O’Shea, *J. Am. Chem. Soc.*, 2005, **127**, 16360–16361.
 - 24 M. Stubbs, P. McSheehy, J. Griffiths and C. Bashford, *Mol. Med. Today*, 2000, **6**, 15–19.
 - 25 A. P. McHale and L. McHale, *Cancer Lett.*, 1988, **41**, 315–321.
 - 26 S. B. Wedam, *et al.*, *J. Clin. Oncol.*, 2006, **24**, 769–777.
 - 27 S. D. Perrault and W. C. W. Chan, *Proc. Natl. Acad. Sci. U. S. A.*, 2010, **107**, 11194–11199.
 - 28 G. F. Paciotti, L. Myer, D. Weinreich, D. Goia, N. Pavel, R. E. McLaughlin and L. Tamarkin, *Drug Delivery*, 2004, **11**, 169–183.
 - 29 H. S. Choi, W. Liu, P. Misra, E. Tanaka, J. P. Zimmer, B. I. Ipe, M. G. Bawendi and J. V. Frangioni, *Nat. Biotechnol.*, 2007, **25**, 1165–1170.